Research Article

Cancer Prevention Research

Cucurbitacin B Alters the Expression of Tumor-Related Genes by Epigenetic Modifications in NSCLC and Inhibits NNK-Induced Lung Tumorigenesis

Samriddhi Shukla[1], Sajid Khan[1], Sudhir Kumar[2], Sonam Sinha[1], Mohd. Farhan[1], Himangsu K. Bora[3], Rakesh Maurya[2,4], and Syed Musthapa Meeran[1,4]

Abstract

Non–small cell lung cancer (NSCLC) represents almost 85% of total diagnosed lung cancer. Studies have shown that combination of DNA methyltransferase (DNMT) and histone deacetylase (HDAC) inhibitors is effective against various cancers, including lung cancer. However, optimizing the synergistic dose regime is very difficult and involves adverse side effects. Therefore, in this study, we have shown that cucurbitacin B (CuB), a single bioactive triterpenoid compound, inhibits both DNMTs and HDACs starting at a very low dose of 60 nmol/L in NSCLC H1299 cells. The CuB-mediated inhibition of DNMTs and HDACs in H1299 cells leads to the reactivation of key tumor suppressor genes (TSG) such as CDKN1A and CDKN2A, as well as downregulation of oncogenes *c-MYC* and *K-RAS* and key tumor promoter gene (TPG), *human telomerase reverse transcriptase* (*hTERT*). The upregulation of TSGs and downregulation of TPG were consistently correlated with the alterations in their promoter methylation and histone modifications. This altered expression of TPG and TSGs is, at least in part, responsible for the inhibition of cellular proliferation and induction of cellular apoptosis in NSCLC. Furthermore, CuB treatment significantly inhibited the tumor incidence and multiplicity in 4-(methylnitrosamino)-1-(3-pyridyl)-1-butanone (NNK)-induced lung tumorigenesis in A/J mice, which was associated with the induction of apoptosis and inhibition of hyperproliferation in the lung tissues. Together, our study provides new insight into the CuB-mediated epigenetic alterations and its chemotherapeutic effects on lung cancer. *Cancer Prev Res; 8(6); 552–62. ©2015 AACR.*

Introduction

Lung cancer is the leading cause of cancer-related mortality worldwide, with nearly 1.4 million deaths each year (1). Non–small cell lung cancers (NSCLC) constitute almost 85% of total diagnosed cases and are caused mainly due to the exposure to the environmental carcinogens. The early stages of lung tumorigenesis involve reversible promoter methylation and histone modification changes (2). Bioactive natural compounds can be defined as the natural compounds that can exhibit a biological activity on the living cells. These compounds possess the capability to reverse the epigenetic alterations. Bioactive natural compounds have been shown to restore the expressions of to tumor suppressor genes (TSG) altered during the course of carcinogenesis (2, 3). Therefore, the uses of bioactive natural compounds have been a major focus of interest as therapeutic options against various classes of diseases, including cancer.

The use of DNA methyltransferase (DNMT) inhibitors alone or in combination with histone deacetylase (HDAC) inhibitors has shown promising results against various cancers through active chromatin modifications (4–7). However, use of synthetic inhibitors invites several limitations, including cost, dose regime, and adverse side effects. Therefore, studies have aimed to use natural DNMT inhibitors alone or in combinations with natural HDAC inhibitors for the prevention and treatment of cancers (7, 8). We have previously shown that dietary combination of green tea polyphenol, a DNMT inhibitor, and sulforaphane, HDAC inhibitor reactivates estrogen receptor (ER)-α in ER-α–negative human breast cancer cells through active chromatin modifications (6). In addition, natural compounds have shown to sensitize the cancer cells for the subsequent treatment with available therapeutics (3, 8). In this study, we explored the epigenetic modulatory activities of cucurbitacin B against NSCLC.

Cucurbitacin B (CuB) is a natural triterpenoid isolated from *Cucurbitaceae* plants, and it has been shown to have anti-plasmodial, immunomodulatory, free-radical scavenging, hepato-protective, cardiovascular, anti-inflammatory, anti-helminthic, and anti-fertility activities (9–12). Recently, there has been growing interest in CuB-mediated anticancer activities, mainly mediated through induction of G_2–M phase cell-cycle arrest, inhibition of the JAK/STAT pathway, and induction of apoptosis (13–19).

[1]Laboratory of Cancer Epigenetics, Division of Endocrinology, CSIR-Central Drug Research Institute, Lucknow, India. [2]Division of Medicinal and Process Chemistry, CSIR-Central Drug Research Institute, Lucknow, India. [3]Division of Laboratory Animals, CSIR-Central Drug Research Institute, Lucknow, India. [4]Academy of Scientific and Innovative Research (AcSIR), New Delhi, India.

Note: Supplementary data for this article are available at Cancer Prevention Research Online (http://cancerprevres.aacrjournals.org/).

Corresponding Author: Syed Musthapa Meeran, Division of Endocrinology, CSIR-Central Drug Research Institute (CSIR-CDRI), Jankipuram Extension, Sector-10, Sitapur Road, Lucknow 226 031, India. Phone: 91-5222772450, ext. 4491; Fax: 91-5222771941; E-mail: s.musthapa@cdri.res.in

doi: 10.1158/1940-6207.CAPR-14-0286

However, these studies have not elucidated the core epigenetic mechanisms behind the anticancer activities of CuB. Our results demonstrate for the first time that CuB, a single bioactive natural compound, exhibits both HDACs and DNMTs inhibitory activities at sub-IC_{50} concentrations in nanomolar range in NSCLC cells. CuB-mediated alterations in histone modifications and promoter methylation lead to induction of TSGs and downregulation of tumor promoter gene (TPG), which results in the inhibition of cellular growth and induction of apoptosis in human NSCLC. Furthermore, CuB treatment significantly inhibited the tumor incidence and multiplicity in 4-(methylnitrosamino)-1-(3-pyridyl)-1-butanone (NNK)-induced lung tumorigenesis in A/J mice, which was associated with the alterations in the expressions of DNMTs and HDACs. This altered expressions of epigenetic enzymes further led to changes in the expression patterns of TSGs, TPG, and oncogenes in the mice lung tissues.

Materials and Methods

Isolation of CuB

CuB was isolated from the fruits of *Luffa graveolense* Roxb. as described in Supplementary Table S1. The structure of CuB was elucidated on the basis of spectroscopic analysis described in Supplementary Table S1, which was in good agreement with that of previously reported (20).

Cell culture and cell proliferation assay

The human NSCLC cells were purchased from ATCC and no authentication was done by the authors except performing a *mycoplasma* test using the LookOut Mycoplasma PCR-detection Kit (Sigma-Aldrich). Cells were cultured and maintained in RPMI-1640 medium supplemented with 10% FBS and 1% penicillin/streptomycin solution in a humidified atmosphere at 37°C with 5% CO_2. CuB was dissolved in ethanol and stored at a stock concentration of 10 mmol/L at 4°C. The maximum final concentration of ethanol in the complete culture medium was less than 0.1% (v/v). Cell proliferation was assayed by standard MTT assay as described previously (6).

Cell-cycle distribution and apoptosis analysis

Approximately 2×10^5 cells were serum-starved overnight and treated with different concentrations of CuB. After 48 hours, cells were harvested and then stained with 50 μg/mL of propidium iodide. Cell-cycle distribution was analyzed using a FACS-Caliber (BD Biosciences). CuB-induced apoptosis in the NSCLC cells were analyzed using the Alexa Fluor 488-Annexin V/Dead Cell Apoptosis Kit (Invitrogen) as described previously (6).

RNA extraction and quantitative real-time PCR

RNA isolation and RT-PCR were performed as described previously (6, 8, 21, 22). The primer sequences and annealing temperatures (T_A) are given in Supplementary Table S2.

Western blot analysis

The procedures have been described previously (6, 21). Briefly, equal amounts of protein were electrophoresced and transferred onto a 0.45-μm polyvinylidene difluoride (PVDF) membrane. Membranes were probed with antibodies against CDKN2A [$p16^{INK4A}$] (SC-1661), CDKN1A [$p21^{CIP1/WAF1}$] (SC-397), DNMT1 (SC-20701), DNMT3a (SC-20703), DNMT3b (SC-10235; Santa Cruz Biotechnology); SIRT3 (ab86671), KAT3B/p300 (ab10485; Abcam); MYC (06-340; Millipore); SIRT2 (12650S), SIRT6 (2590), HDAC 1-6 (9928S), RAS (3965), CBP, GCN5L2, PCAF (8686S), and β-actin (Cell Signalling). The membranes were then incubated with respective secondary antibody. Immunoreactive bands were visualized using the Enhanced Chemiluminescence Detection System.

HDACs and DNMTs activity assays

The HDACs and DNMTs activities were analyzed using the colorimetric assay kits (Active Motif) as described previously (21, 22).

Southwestern dot-blot analysis

The effect of CuB treatment on the degree of genomic methylation was determined using dot-blot analysis, as described previously (6). Briefly, 1 μg of gDNA was transferred onto a nitrocellulose membrane and fixed by baking the membrane for 1 hour at 80°C. After blocking the nonspecific binding sites, the membrane was incubated with the anti-5-methyl cytosine (5-mC) antibody (MABE146; Millipore) for 2 hours. Furthermore, the membrane was incubated with horseradish peroxidase (HRP)-conjugated secondary antibody and bands were visualized using chemiluminescence detection system.

Methylation-specific PCR assay

The DNA methylation statuses of the $p21^{CIP1/WAF1}$ and *hTERT* promoters were assessed by MSP using the EpiTect Bisulfite Modification Kit (Qiagen) following the manufacturer's protocol. After 48 hours of CuB treatment, 2 μg of gDNA was bisulfite converted and then PCR amplified using the Platinum Taq polymerase (Invitrogen). MSP primer sequences and respective annealing temperatures are given in Supplementary Table S3.

Chromatin immunoprecipitation assay

Chromatin immunoprecipitation (ChIP) assays were performed using the EZ-ChIP Kit according to the manufacturer's protocol (Millipore) as described previously (21, 22). The antibodies used in the ChIP assays were ChIP-validated anti-acetyl histone H3 (06-599), anti-acetyl histone H4 (06-598), anti-acetyl histone H3K9 (07-352), anti-histone H3K9me3 (07-442), anti-histone H3K27me3 (07-449; Millipore) and anti-MeCP2 (ab2828; Abcam). Input DNA was used as an internal control. No antibody control was used to check ChIP efficiency. ChIP-purified DNA was amplified by PCR and the reaction was initiated at 94°C for 5 minutes followed by 25 cycles of PCR (94°C, 30 seconds; T_A°C, 30 seconds; 72°C, 30 seconds) and extended at 72°C for 5 minutes. The promoter regions of $p16^{INK4A}$ were amplified using touchdown PCR. The primer sequences and conditions are given in Supplementary Table S3.

Animal experiments

Female A/J mice, 5 to 6 weeks old, were procured and handled according to the protocol approved by the Institutional Animal Ethics Committee, CSIR-CDRI. Mice were randomized into 4 groups ($n = 8$); three groups were injected i.p. with NNK dissolved in saline [Sigma; 100 mg/kg body weight (b.w)] and the control group was injected with saline as vehicle once a week for 2 consecutive weeks. On third week onward, NNK-administrated mice were treated with 0.1 or 0.2 mg/kg b.w. of CuB through i.p. twice a week for 10 weeks. CuB was dissolved in ethanol at a stock concentration of 5 mg/mL and diluted in PBS on the day of use. The maximum concentration of ethanol was less than 0.1% and

the control mice were treated with the vehicle. After 13th week, CuB treatment was stopped and the mice were left untreated until they were sacrificed. At 21st week, mice were sacrificed and examined for tumor incidence, multiplicity, and lung wet weight.

Immunohistochemical staining

Formalin-fixed lung tissue sections (5 μm) were processed for hematoxylin and eosin (H&E) staining. Three H&E sections, at least 600 μm apart, were analyzed blindly by a veterinary pathologist for different histopathologic lesions and graded according to the recommendations of the Mouse Models of Human Cancer Consortium as described previously (23, 24). The histopathologic lesions were scored on the basis of severity, from 0 to 4: grade 0: absent, lesions affect less than 5% of tissue; grade 1:mild, lesions affect 6%–20% of tissue; grade 2: moderate, lesions affect 21%–40% of tissue; grade 3: severe, lesions affect 41%–75% of tissue; and grade 4: extensive, lesions affect 76%–100% of tissue. Immunohistochemical analysis of proliferating cell nuclear antigen (PCNA) and terminal deoxynucleotidyl transferase–mediated dUTP nick end labeling (TUNEL) assays were performed as described previously (25). The numbers of PCNA- and TUNEL-positive cells were counted in at least 6 different microscopic fields as the average number of positive cells × 100/total number of cells.

Statistical analysis

Statistical significance of differences between the values of untreated controls and CuB-treated groups was determined with one-way ANOVA using Dunnet's multiple comparison test on GraphPad Prism version 5.00 for Windows. In each case, $P < 0.05$ was considered statistically significant.

Results

CuB inhibits cellular proliferation and induces cellular apoptosis

To determine the effective dose of CuB on human NSCLC cells, we performed cellular proliferation, cell-cycle arrest, and apoptosis analyses. We observed a dose- and time-dependent inhibition of cellular proliferation with CuB treatment in A549, H1299, and H1650 cells as shown in Supplementary Fig. S1A. Inhibition of cell growth was more prominent in the $p53^-$ H1299 cells as compared to $p53^+$ A549 cells and $p53^+$ $EGFR^-$ H1650 cells (Fig. 1A). As shown in Fig. 1A–C, CuB significantly inhibited cellular proliferation and induced cellular apoptosis as well as G_2–M phase cell-cycle arrest in H1299 cells at an IC_{50} concentration of 60 nmol/L ($P < 0.05$) and onward, therefore further detailed analysis of molecular mechanism of its action was performed in this cell line with 60 nmol/L as median concentration. In addition to H1299 cells, A549 cells also showed dose-dependent G_2–M phase cell-cycle arrest and induction of cellular apoptosis with CuB treatment (Supplementary Fig. S1B and S1C).

CuB alters the expression of key tumor-related genes

As shown in Fig. 1D, CuB at concentrations of 60 nmol/L or higher significantly increased the mRNA and proteins expression of key cell-cycle regulatory TSGs such as $p16^{INK4A}$ and $p21^{CIP1/WAF1}$ in H1299 cells. However, we found slightly decreased mRNA expressions of these TSGs at 600 nmol/L as compared with 60 nmol/L CuB concentrations, which might be due to the mRNA instability as well as higher rate of protein turnover observed in case of cell-cycle regulators (26, 27). Overall, these mRNA and protein expressions are consistently upregulated by the CuB treatment in H1299 cells irrespective of dose responses. Treatment with CuB in H1299 cells downregulated the protein expressions of oncogenes, c-MYC, and K-RAS; however, their mRNA expressions were not altered significantly (Fig. 1E). As shown in (Fig. 1F), CuB treatment significantly reduced the expression of *hTERT*, the catalytic subunit of telomerase, starting with a dose of 6 nmol/L onwards at 48 hours. Therefore, these results suggest that the antiproliferative and proapoptotic effects of CuB are, at least in part, associated with the altered expressions of key tumor-related genes in NSCLC cells.

CuB altered the expression and activity of epigenetic modulatory enzymes

Genetic alterations are accompanied by epigenetic modulations during carcinogenesis (2, 6). Hence, we analyzed the expressions of both types of DNMTs, maintenance methyltransferase DNMT1, and *de novo* methyltransferases, DNMT3a and DNMT3b. As shown in Fig. 2A, CuB treatment significantly inhibited the expressions of *DNMT1* and *DNMT3b* starting from CuB concentrations of 600 nmol/L or higher in H1299 cells. Interestingly, the protein expressions of all the 3 DNMTs were drastically reduced starting from IC_{50} concentration of CuB in H1299 cells (Fig. 2B). Furthermore, we have also observed a significant inhibition of DNMTs activity starting with the CuB concentrations of 200 nmol/L in another NSCLC A549 cell line (Supplementary Fig. S1D). In addition to DNMTs, HDACs, especially HDAC1, HDAC5, and HDAC6 were found to be considerably downregulated by CuB starting with 60 nmol/L concentrations in H1299 cells. NAD^+-dependent class III HDACs, SIRT3, and SIRT6 were also found to be downregulated at 60 nmol/L or higher concentrations of CuB. We further analyzed the protein expressions of different histone acetyltransferases (HAT) such as CBP, GCN5L2, PCAF, and p300 after CuB treatment in H1299 cells for 48 hours. We found that CBP and PCAF expressions were marginally upregulated at sub-IC_{50} and IC_{50} concentrations of CuB (Fig. 2C). Furthermore, CuB not only inhibited the expressions but also dose dependently inhibited the activity of HDACs in NSCLC cells (Fig. 2D; Supplementary Fig. S1D).

As we found that the treatment of H1299 cells with CuB inhibited the expression of DNMTs, we further investigated the consequence of their inhibition at the extent of global as well as gene-specific promoter methylation. Treatment of CuB in H1299 cells resulted in a significant dose-dependent reduction in 5-mC levels, a marker for global DNA methylation (Supplementary Fig. S2A). Furthermore, as shown in Supplementary Fig. S2B, gene-specific promoter methylation of $p21^{CIP1/WAF1}$ and *hTERT* was also found to be significantly downregulated at 60 nmol/L of CuB concentration in H1299 cells.

CuB altered histone modifications at the $p16^{INK4A}$, $p21^{CIP1/WAF1}$, and *hTERT* promoters

ChIP assays were performed to investigate CuB-mediated changes in binding of various active and inactive chromatin marks at the $p16^{INK4A}$, $p21^{CIP1/WAF1}$, and *hTERT* promoters. As shown in Fig. 3A, we designed 5 sets of primers for the CpG-rich $p16^{INK4A}$ promoter regions upstream of the transcription start site. There are 2 Alu sites in the amplicons of the distal primers, ChIP 1 and ChIP 2, which are densely methylated and transcriptionally inactive. Therefore, the proximal promoter regions amplified by ChIP 3-5 more actively participate in the transcriptional activation of $p16^{INK4A}$. As shown in Fig. 3B and C, we selected 3 different

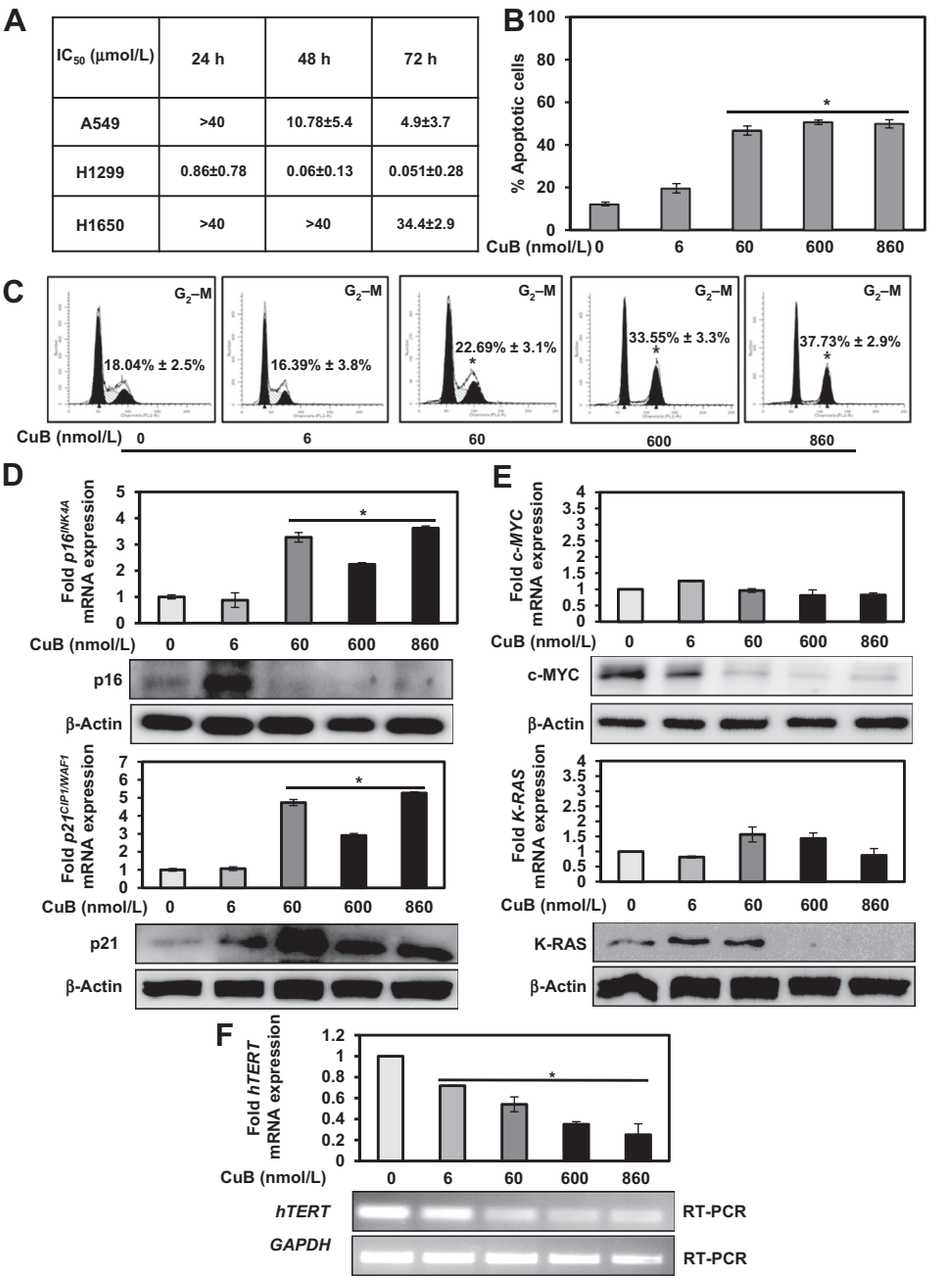

Figure 1.
CuB inhibits cellular proliferation and induces apoptosis as well as alters the expression of key tumor-related genes in human NSCLC cells. A, IC_{50} values of CuB (0.01–40 μmol/L)-treated NSCLC cells at 24, 48, and 72 hours. B, treatment with CuB at indicated doses for 48 hours induced cellular apoptosis in H1299 cells. The graphical representation shows the percentage of total apoptotic cells. C, CuB-induced G_2–M phase cell-cycle arrest in H1299 cells at 48 hours. The values are mean ± SE of cells in G_2–M phase. D and E, effect of CuB treatment (0–860 nmol/L) on the mRNA and protein expressions of *$p16^{INK4A}$*, *$p21^{CIP1/WAF1}$*, *c-MYC*, and *K-RAS* at 48 hours in H1299 cells. F, effect of CuB treatment on the mRNA expressions of *hTERT* at 48 hours. The values were plotted as relative fold mRNA expression and were normalized to *GAPDH*. The protein expressions at similar treatment conditions are shown under respective real-time mRNA expression results with β-actin as an equal loading control. Results represent mean of 3 independent experiments (mean ± SE). Significance against respective control. *, $P < 0.05$.

histone acetylation marks such as acetyl histone 3 (AcH3), acetyl histone 4 (AcH4), and acetylation at lysine 9 of histone 3 (AcH3K9) as active chromatin marks. We found significantly higher enrichment of AcH3 at both proximal and distal promoters of *$p16^{INK4A}$* in H1299 cells after 48 hours of CuB treatment. This observation indicates that the HDAC inhibitory activity of CuB (Fig. 2D) leads to histone hyperacetylation especially in case of histone 3. The enrichment of AcH4 was almost unaltered except for the 2-fold increase in ChIP 3. Furthermore, we also found a significant decrease in the methylation status of inactive chromatin marks such as trimethylation at lysine 9 of histone 3 (H3K9me3) and trimethylation at lysine 27 of histone 3 (H3K27me3) at proximal regions (ChIP 3-5) of the *$p16^{INK4A}$* promoter in H1299 cells with CuB treatment.

In case of the *$p21^{CIP1/WAF1}$* promoter, we designed 2 distinct sets of primers for 2 functionally important regions of the distal promoter as shown in Fig. 4A. The primer pair amplifying ChIP 1 flanks a sp1-binding site on the *$p21^{CIP1/WAF1}$* promoter. Enrichment of AcH3 was found to be significantly increased at CuB concentrations of 6 and 60 nmol/L ($P < 0.05$), whereas the enrichment of AcH4 and AcH3K9 showed no significant alteration at both the promoter sites (Fig. 4B and C). Binding of inactive chromatin marks such as H3K9me3 and H3K27me3 at the *$p21^{CIP1/WAF1}$* ChIP 1 promoter region was decreased

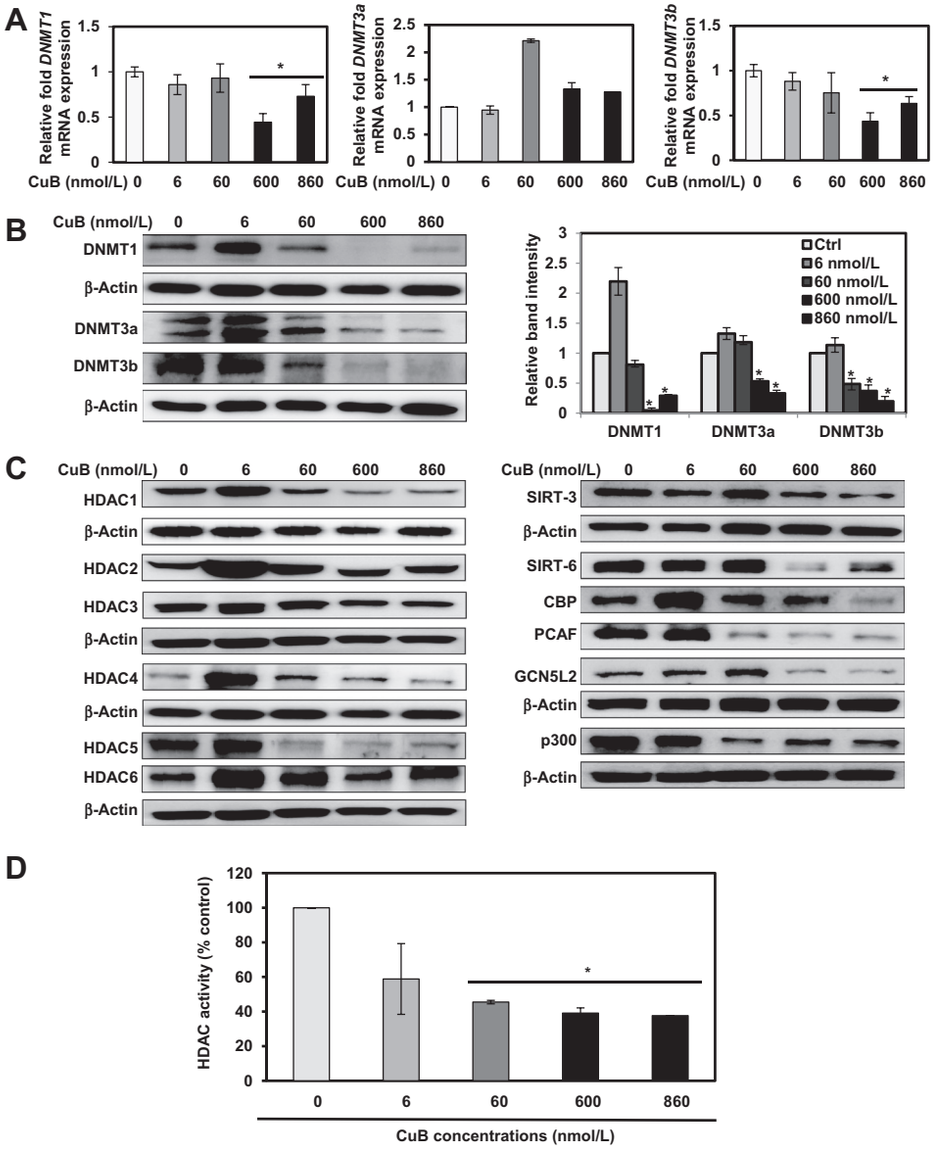

Figure 2.
CuB inhibits epigenetic modulatory enzymes. A, effect of CuB treatment on the mRNA expressions of *DNMTs* in H1299 cells after 48 hours. The values are normalized to *GAPDH*. B, treatment of H1299 cells with CuB for 48 hours altered the levels of protein expression of DNMTs. Graphical representations are indicative of relative band intensities. C, effect of CuB treatment on the protein expressions of HDACs, SIRTs, and HATs at 48 hours in H1299 cells. β-Actin was used as an equal loading control. D, H1299 cells were treated with indicated concentrations of CuB for 48 hours and nuclear extracts were assessed for HDACs activity. The values are mean ± SE. *, $P < 0.05$ against respective control.

significantly with CuB treatment. Furthermore, our results also evidenced a p53-independent $p21^{CIP1/WAF1}$ upregulation with CuB treatment in $p53^{-}$ H1299 cells.

Similarly, we designed 5 sets of primers for the *hTERT* promoter spanning the regions from distal promoter to the first exonic region (Fig. 5A). As shown in Fig. 5B and C, the relative enrichment of AcH3 was increased in a range between 1.5- and 5.5-fold ($P < 0.05$) in CuB-treated H1299 cells at sub-IC_{50} and IC_{50} concentrations, respectively, starting from distal to proximal promoters of *hTERT*. The other 2 active acetylation marks AcH4 and AcH3K9 showed a marginal increase in enrichment at some of the promoter regions in the *hTERT*. In accordance with histone acetylation, histone methylation marks were also enriched up to 1.5- to 2.5-fold ($P < 0.05$) at distal as well as proximal promoter regions of *hTERT*. The enrichment of MeCP2 was found to be increased at the distal promoter sites (ChIP 1 and ChIP 2) and first exonic region (ChIP 5) in a range lying between 2.5- and 3.6-fold ($P < 0.05$) higher than the untreated H1299 cells. The proximal promoter and first exonic region of *hTERT* have binding sites for many important transcription factors and preoccupancy of these sites with inactive chromatin marks might hinder their binding to the *hTERT* promoter leading to the downregulation of *hTERT* expression (21). Furthermore, we observed a significant disruption of the enrichment of c-MYC at the selected regions of *hTERT* promoter after CuB treatment in H1299 cells (Fig. 5B and C). Collectively, these results suggest that the CuB-mediated chromatin modifications are, at least in part, responsible for the altered expressions of $p16^{INK4A}$, $p21^{CIP1/WAF1}$, and *hTERT* in H1299 cells.

CuB inhibits NNK-induced lung tumorigenesis

Next, we sought to determine the effect of CuB on NNK-induced lung tumorigenesis. The schematic experimental design

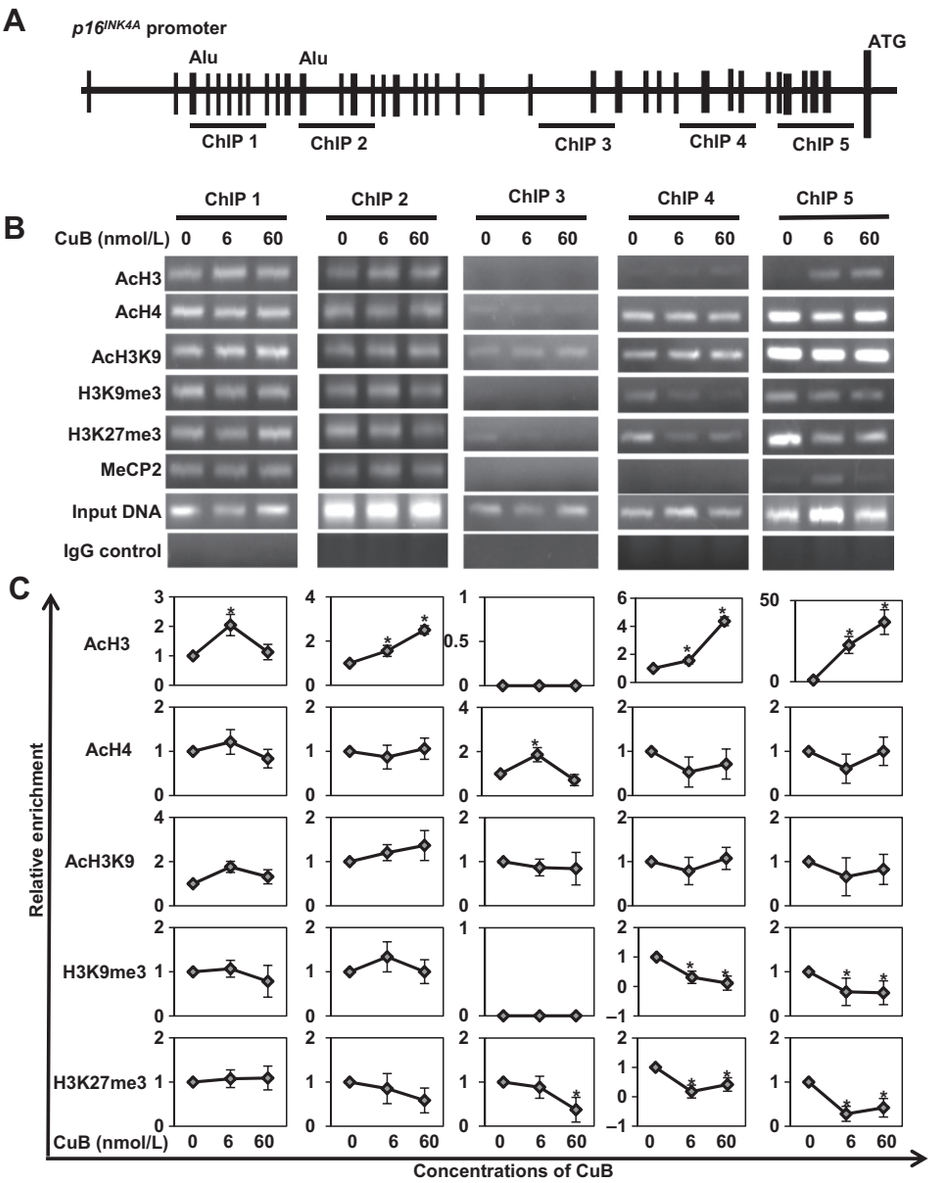

Figure 3.
CuB induced histone modification changes at the *p16*^{INK4A} promoter. A, schematic representation of different CpG-rich regions (represented as ChIP 1–5) of the *p16*^{INK4A} promoter, upstream of the transcription start site. B, H1299 cells were treated with the indicated concentrations of CuB for 48 hours and analyzed by ChIP-PCR assays for the enrichment of different chromatin markers at the *p16*^{INK4A} promoter. Input DNA was used as control. IgG control was used as negative control. The gel images are representatives of 3 independent experiments. C, The *x*-axes represent CuB concentrations in nmol/L, and the *y*-axes represent the relative enrichment of individual histone modifications and binding factors, the percentage of untreated immunoprecipitates compared with the corresponding input samples (defined as 1) at different primer positions. Each point indicates the mean ± SE. *, $P < 0.05$ against respective control.

is given in Fig. 6A. We found no significant difference in the average body weights of mice in the individual groups (Supplementary Fig. S3A). Histopathologic examination revealed that the lungs of NNK-induced mice showed a highest grade of bronchiolar and alveolar hyperplasia, adenocarcinoma, and microadenomas compared with the lungs of vehicle-treated control mice (Fig. 6B; Supplementary Fig. S3B and Supplementary Table S4). Tumor angiogenesis, which is marked by the formation of new and irregular blood vessels, was also prevalent in the NNK-induced lungs, which decreased dose dependently in CuB-treated groups (Fig. 6B; Supplementary Fig. S3B and Supplementary Table S4). As shown in Fig. 6C, NNK-administrated mice had significantly higher incidence of lung cancer (100%) and tumor multiplicity (17.75 ± 7.4 lung tumors per mouse) compared with vehicle-administered control mice. Interestingly, treatment with CuB resulted in a significantly reduced tumor incidence and tumor multiplicity compared with vehicle-treated NNK-induced lung tissues (Fig. 6C).

Furthermore, as shown in Fig. 6D, the presence of PCNA was highest in the NNK-administrated control lungs. The percentage of PCNA-positive cells was significantly ($P < 0.01$) lowered in 0.1 and 0.2 mg/kg b.w. CuB-treated mice lungs as compared with NNK-administrated vehicle-treated mice lungs. Next, we sought to determine the effect of CuB on cell death in NNK-induced lung cancer using TUNEL assay. Immunohistochemical analysis revealed a significantly higher number of TUNEL-positive cells at 0.1 and 0.2 mg/kg b.w. CuB-treated mice lungs compared with NNK-induced mice lungs (Fig. 6D). Overall, CuB-inhibited hyperproliferation and enhanced cell death in NNK-induced hyperproliferative lung cancer in A/J mice.

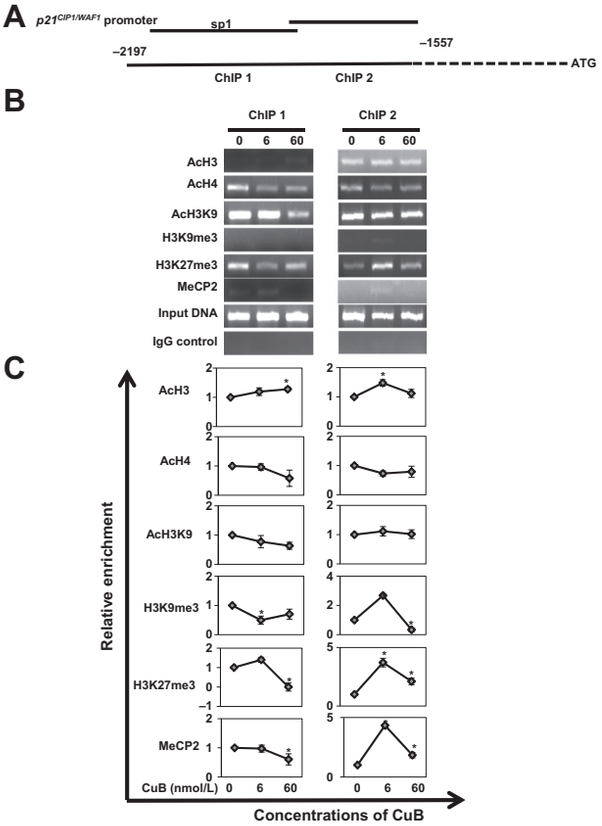

Figure 4.
CuB induced histone modification changes at the $p21^{CIP1/WAF1}$ promoter. A, schematic representation of amplicons for 2 different CpG-rich regions (represented as ChIP1 and ChIP2) of the $p21^{CIP1/WAF1}$ promoter. B, H1299 cells were treated with the indicated concentrations of CuB for 48 hours and analyzed by ChIP-PCR for the enrichment of different chromatin markers at the $p21^{CIP1/WAF1}$ promoter. Input DNA was used as control. IgG control was used as a negative control. The gel images are representatives of 3 independent experiments. C, the *x*-axes represent CuB concentrations in nmol/L, and the *y*-axes represent the relative enrichment of individual binding factors. Each point indicates the mean ± SE. *, $P < 0.05$ against respective control.

CuB alter the expressions of epigenetic enzymes and tumor-related genes in NNK-induced lung tissues

To further validate our *in vitro* results, we analyzed the expressions of epigenetic modulatory enzymes in the CuB-treated and untreated NNK-induced mice lungs. As shown in the Fig. 6E, CuB treatment led to decreased protein expressions of DNMTs. The DNMT inhibitory effects were more pronounced at 0.2 mg/kg b.w. CuB dose. Similarly, CuB also inhibited the protein expression of different HDACs (HDACs 1–4), with considerably higher inhibition of HDACs expression at 0.2 mg/kg b.w. CuB dose. Furthermore, we have observed that CuB-induced significant upregulation of $p16^{INK4A}$ and $p21^{CIP1/WAF1}$, which is consistent with our *in vitro* results. However, we also found a significantly increased expression of $p16^{INK4A}$ in the NNK-induced group (Fig. 6F). The expression of tumor promoter *Tert* was significantly inhibited in 0.1 and 0.2 mg/kg b.w. CuB-treated animal groups, further validating our *in vitro* results (Fig. 6F). In accordance, we have also observed a considerable downregulation of the expressions of oncogenes c-MYC and RAS in CuB-treated mice lungs compared with NNK-induced lung tissue (Fig. 6F).

Discussion

The upregulation of TSGs and downregulation of TPGs have been causally linked with the inhibition of cellular proliferation and induction of cellular apoptosis (4, 8, 28). In our present study, treatment of NSCLC cells with CuB-induced upregulation of key TSGs and downregulation of oncogenes as well as TPGs. There are multiple epigenetic mechanisms, such as promoter methylation, chromatin modifications, and miRNA-mediated silencing, that are involved in the alterations of gene expressions (21, 22, 28, 29). Therefore, we evaluated the CuB-mediated epigenetic modifications, including changes in the global as well as gene-specific methylation and histone modifications in NSCLC cells. Interestingly, we found that CuB inhibited the expression of both DNMTs and HDACs in these cells. Previous studies have shown that treatment with either DNMTs inhibitor alone or in combination with HDACs inhibitor altered the expressions of TSGs and TPGs in many cancers (3, 21, 28, 30). In general, promoter regions of the TSGs are hypermethylated causing their silencing in cancer and treatment with DNMTs inhibitor has been shown to reactivate their expression by altering their methylation status (28). In contrast, hypermethylation at *hTERT* promoter is associated with transcriptional activation by inhibiting the binding of various methylation-sensitive transcriptional repressor proteins (21, 31). Together, our results suggest that CuB-induced downregulation of DNMTs not only facilitated the expression of TSGs but also inhibited the expression of *hTERT* in H1299 cells.

In addition to alterations in DNA methylation, chromatin modifications also play major role in gene regulation in cancers. In general, HDACs are frequently overexpressed in many cancers, and inhibition of HDACs induces re-expression of epigenetically silenced genes (7, 8, 28). Our results suggest that CuB-mediated HDACs inhibition altered the accessibility of various transcriptional factors to the promoters of the TSGs and TPG in H1299 cells. Furthermore, we also observed that CuB at 6 nmol/L concentration induced both class I and class II HDACs, which seems to be the cellular survival strategy to combat with the autophagic effects of CuB (32, 33). The protein expressions of HATs, PCAF, and CBP were increased after CuB treatment, which might also help in inducing the expressions of the TSGs, as reported previously (34, 35).

The changes in the expression and activities of epigenetic modulatory enzymes lead to alterations in histone modifications. In general, the acetylation at H3K9 results into gene activation, whereas methylation at H3K9 (H3K9me3) results into gene repression (2, 28, 36). It is a well-established fact that the sites and degree of histone methylation define its role in gene regulation (37). The sites with higher enrichment of histone methylation marks, H3K9me3 and H3K27me3, represent transcriptionally inactive regions of chromatin. We found significantly lowered enrichment of these histone methylation marks at the promoters of TSGs, whereas their enrichment was increased at the *hTERT* promoter after CuB treatment in H1299 cells. Many HDACs inhibitory compounds have shown p53-independent $p21^{CIP1/WAF1}$ upregulation (38, 39), which again validates the HDACs inhibitory nature of CuB.

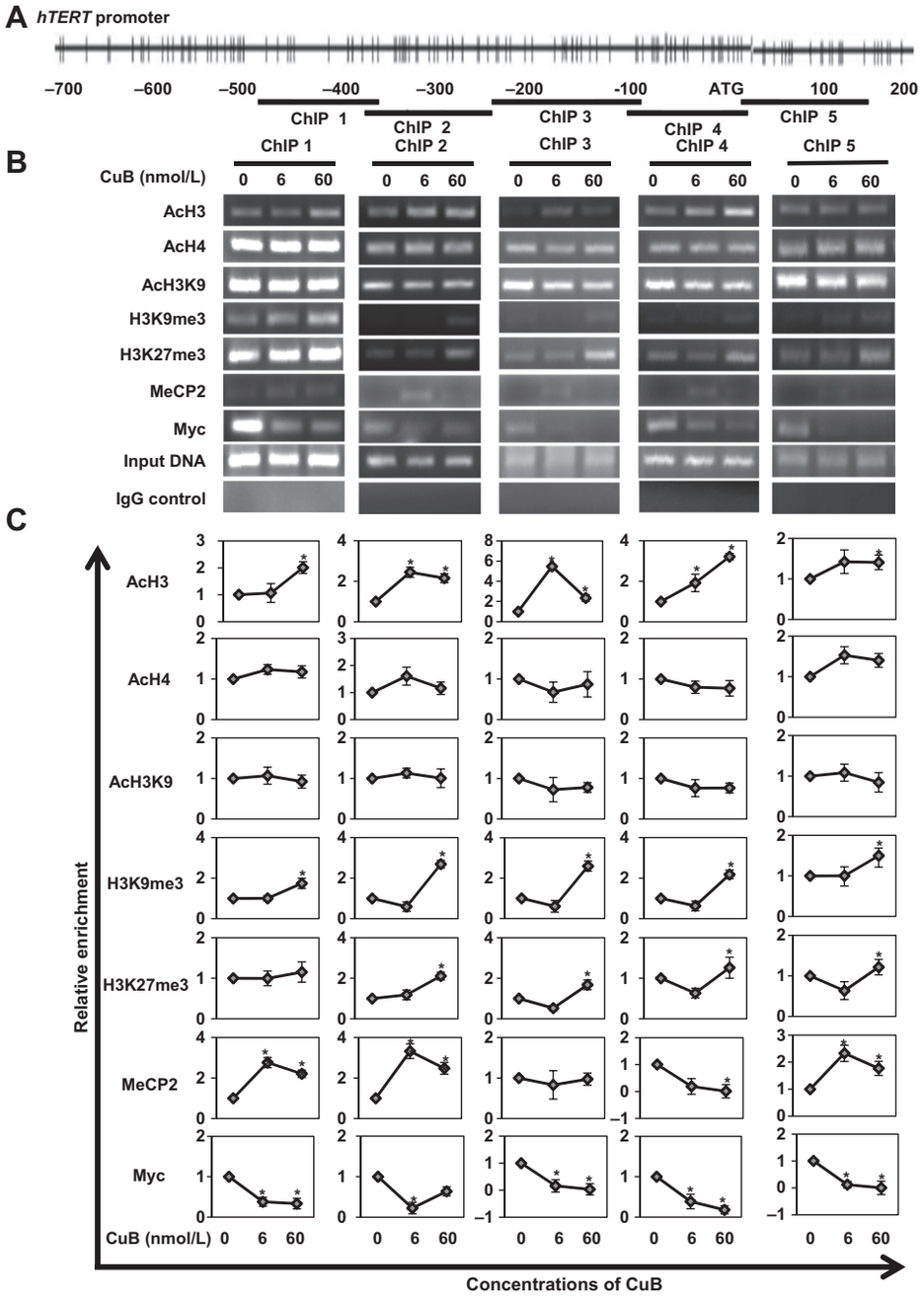

Figure 5.
CuB alters the enrichment of different histone modification marks at the *hTERT* promoter. A, schematic representation of amplicon for different CpG-rich regions (represented as ChIP 1–5) of the *hTERT* promoter, spanning from distal promoter to the first exonic region. B, H1299 cells were treated with the indicated concentrations of CuB for 48 hours and analyzed for the binding of various chromatin marks and transcriptional factors in the promoter region of *hTERT*. Input DNA samples were used as control. IgG control was used as a negative control. The gel images are representatives of 3 independent experiments. C, the *x*-axes represent CuB concentrations in nmol/L, and the *y*-axes represent the relative enrichment of individual binding factors compared with the corresponding input samples (defined as 1). Each point indicates the mean ± SE. *, $P < 0.05$ against respective control.

Methyl-CpG–binding domain proteins (MBD) form a nuclear DNA-binding protein family comprising MBD 1-4 and MeCP2. These proteins are capable of binding specifically to methylated DNA and are known to be involved in DNA methylation–mediated transcriptional repression (2). Binding of MeCP2 to the selected promoter regions of the $p21^{CIP1/WAF1}$ was significantly disrupted following CuB treatment, whereas at the *hTERT* promoter sites, MeCP2 binding was found to be increased. Furthermore, we have also found a higher enrichment of active chromatin marks at the $p16^{INK4A}$ and $p21^{CIP1/WAF1}$ promoters and a higher enrichment of inactive chromatin marks at the *hTERT* promoter, which facilitate alterations in their expressions (21–22, 28, 31). Furthermore, CuB-mediated downregulation of c-MYC expression facilitates the disruption of the binding of c-MYC, a transcription activator of *hTERT*, to the *hTERT* promoter in H1299 cells. On the other hand, c-MYC represses $p21^{CIP1/WAF1}$ expression by forming complexes with transcription factors Sp1/Sp3, which are required for its expression. Because of CuB-mediated inhibition, c-MYC becomes incapable of binding to the transcription factors Sp1/Sp3, which are required to bind to the $p21^{CIP1/WAF1}$

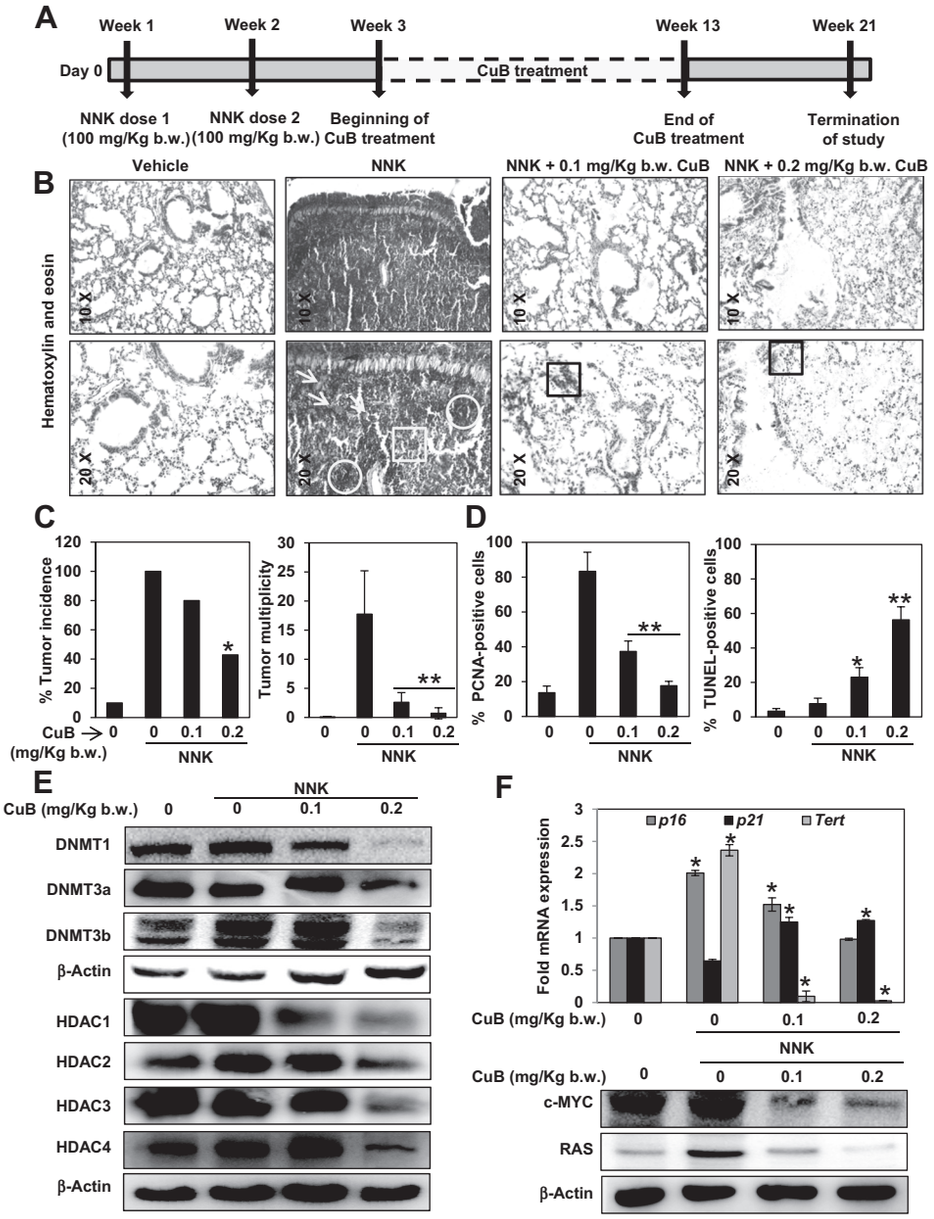

Figure 6.
CuB inhibited NNK-induced lung tumorigenesis in A/J mice. A, schematic representation of the experimental protocol used to study the effects of CuB on NNK-induced lung carcinogenesis in A/J mice. B, representative lung histology (10× and 20×) of different animal groups using H&E staining. The arrows represent angiogenesis; circles represent microadenomas; and squares represent tumor hyperplasia. C, the percentages of tumor incidence and tumor multiplicity of indicated animal groups are plotted. Columns, mean ($n = 8$); bars, SD. D, percentage of PCNA- and TUNEL-positive cells in the lung sections of different animal groups. Columns, mean ($n = 8$); bars, SD. *, $P < 0.05$; **, $P < 0.01$, significant against the NNK-induced control group. E, effect of CuB treatment on the protein expressions of different DNMTs and HDACs in mouse lung tissue. β-Actin was used as an equal loading control. The blots are representative of 3 independent experiments. F, effect of CuB treatment on the mRNA expressions of $p16^{INK4A}$, $p21^{CIP1/WAF1}$, and *Tert* as well as protein expressions of c-MYC and RAS in the mouse lung tissue. For mRNA expressions, the values were plotted as relative fold mRNA expression and were normalized to *Gapdh*. The results are means ± SE. *, $P < 0.05$, significant against the vehicle-treated control group.

promoter to facilitate its activation (40). The downregulation of c-MYC, due to the CuB treatment, thus indirectly leads to the upregulation of the $p21^{CIP1/WAF1}$. On the basis of these observations, we propose that CuB-mediated upregulation of $p21^{CIP1/WAF1}$ and downregulation of *hTERT* is, at least in part, mediated through alterations in promoter methylation and chromatin modifications in NSCLC.

NNK has been shown to induce lung carcinogenesis through both genetic and epigenetic mechanisms. Early changes during NNK-induced lung carcinogenesis include altered expression of DNMT1 and HDACs (41, 42). Because CuB was found to alter the expression of DNMTs and HDACs *in vitro*, we selected an NNK-induced lung cancer mice model to assess the *in vivo* lung anticancer potential of CuB. In previous studies, the use of combinations of 0.1 mg/kg b.w. 5-aza-2′-deoxycytidine, a standard DNMT inhibitor, and 400 mg/kg b.w. valproic acid, a standard HDAC inhibitor, have been reported to cause a moderate reversible leukocytopenia in mice (43). In yet another study performed in rats, the combinations of 20 mg/kg b.w. SGI-110, a DNMT inhibitor along with 1 mg/kg b.w. entinostat, a HDAC inhibitor also resulted in a significant weight loss in the animals (44). In contrast, CuB doses used in this study inhibited the expressions of both DNMTs and HDACs *in vivo* with no visible sign of toxicity in the animals. Furthermore, alterations in the expressions of these epigenetic modulatory enzymes facilitate the upregulation of TSGs and downregulations of oncogenes as well as TPG as observed *in vitro*. Expression of $p16^{INK4A}$ is transcriptionally silenced in H1299 cells, whereas it was highly upregulated in the

NNK-induced lung tissues in A/J mice. In contrast to the *in vitro* results, CuB was found to downregulate NNK-induced $p16^{INK4A}$ upregulation, which might be due to the dysfunctional downstream Rb phosphorylation pathway resulting in the inability of the $p16^{INK4A}$ to inhibit the cellular proliferation in NNK-induced tumors (45). However, CuB-mediated upregulation of other TSGs such as $p21^{CIP1/WAF1}$ and downregulation of TPGs leads to the inhibition of NNK-induced lung tumorigenicity. Furthermore, we have also observed that CuB effectively reduced the severity of the NNK-induced lung tumorigenesis by inhibiting tumor incidence, multiplicity, and lung hyperplasia, which is well correlated with the inhibition of PCNA and induction of apoptotic cells in the CuB-treated NNK-induced lung tumors.

Our study is the first of its kind to show the efficacy of CuB against NNK-induced lung tumors. As per our knowledge, this is the first report showing CuB-mediated inhibition of both DNMTs and HDACs and its epigenetic mechanism of action both *in vitro* and *in vivo*. This finding becomes even more significant due to the strong anticancer activity exhibited by a low concentration of CuB against NSCLC. In conclusion, our results suggest that CuB could be developed as a very potent lung anticancer molecule and it could also be used in designing novel epigenetic therapeutic strategy against NSCLC in humans.

Disclosure of Potential Conflicts of Interest

No potential conflicts of interest were disclosed.

Authors' Contributions

Conception and design: S. Shukla, R. Maurya, S.M. Meeran

Development of methodology: S. Shukla, S. Khan, S. Kumar, S. Sinha, M. Farhan, H.K. Bora

Acquisition of data (provided animals, acquired and managed patients, provided facilities, etc.): S. Shukla, S. Khan, S. Kumar, S. Sinha, M. Farhan, H.K. Bora, S.M. Meeran

Analysis and interpretation of data (e.g., statistical analysis, biostatistics, computational analysis): S. Shukla, S. Khan, S. Kumar, S.M. Meeran

Writing, review, and/or revision of the manuscript: S. Shukla, S. Khan, R. Maurya, S.M. Meeran

Administrative, technical, or material support (i.e., reporting or organizing data, constructing databases): S.M. Meeran

Study supervision: R. Maurya, S.M. Meeran

Other (isolation and characterization of CuB): R. Maurya

Acknowledgments

Senior research fellowships to S. Shukla, S. Khan, and S. Kumar from the CSIR and UGC is acknowledged. Technical assistance from Jyoti Verma and Amar Deep Lakra is also gratefully acknowledged. The authors thank A.L. Vishwakarma from the division of SAIF, CSIR-CDRI for FACS analysis. CSIR-CDRI communication # 8947.

Grant Support

This work was supported by funds from the CSIR-EpiHeD-Network Scheme (BSC0118), Science & Engineering Research Board (SR/FT/LS-80/2011), and Department of Biotechnology-Twinning Programme (BCIL/NER-BPMC/2013/722), New Delhi, India, to S.M. Meeran.

The costs of publication of this article were defrayed in part by the payment of page charges. This article must therefore be hereby marked *advertisement* in accordance with 18 U.S.C. Section 1734 solely to indicate this fact.

Received August 29, 2014; revised March 5, 2015; accepted March 22, 2015; published OnlineFirst March 26, 2015.

References

1. Jemal A, Bray F, Center MM, Ferlay J, Ward E, Forman D. Global cancer statistics. CA Cancer J Clin 2011;61:69–90.
2. Shukla S, Khan S, Tollefsbol TO, Meeran SM. Genetics and epigenetics of lung cancer: mechanisms and future perspectives. Curr Cancer Ther Rev 2013;9:97–110.
3. Meeran SM, Ahmed A, Tollefsbol TO. Epigenetic targets of bioactive dietary components for cancer prevention and therapy. Clin Epigenetics 2010;1:101–16.
4. Fang MZ, Wang Y, Ai N, Hou Z, Sun Y, Lu H, et al. Tea polyphenol (-)-epigallocatechin-3-gallate inhibits DNA methyltransferase and reactivates methylation-silenced genes in cancer cell lines. Cancer Res 2003;63:7563–70.
5. Jha AK, Nikbakht M, Parashar G, Shrivastava A, Capalash N, Kaur J. Reversal of hypermethylation and reactivation of the RARbeta2 gene by natural compounds in cervical cancer cell lines. Folia Biol 2010;56:195–200.
6. Meeran SM, Patel SN, Li Y, Shukla S, Tollefsbol TO. Bioactive dietary supplements reactivate ER expression in ER-negative breast cancer cells by active chromatin modifications. PLoS One 2012;7:e37748.
7. Myzak MC, Ho E, Dashwood RH. Dietary agents as histone deacetylase inhibitors. Mol Carcinog 2006;45:443–6.
8. Li Y, Chen H, Hardy TM, Tollefsbol TO. Epigenetic regulation of multiple tumor-related genes leads to suppression of breast tumorigenesis by dietary genistein. PLoS One 2013;8:e54369.
9. Alghasham AA. Cucurbitacins - a promising target for cancer therapy. Int J Health Sci 2013;7:77–89.
10. Chen JC, Chiu MH, Nie RL, Cordell GA, Qiu SX. Cucurbitacins and cucurbitane glycosides: structures and biological activities. Nat Prod Rep 2005;22:386–99.
11. Attard E, Brincat MP, Cuschieri A. Immunomodulatory activity of cucurbitacin E isolated from Ecballium elaterium. Fitoterapia 2005;76:439–41.
12. Chen C, Qiang S, Lou L, Zhao W. Cucurbitane-type triterpenoids from the stems of Cucumis melo. J Nat Prod 2009;72:824–9.
13. Chen W, Leiter A, Yin D, Meiring M, Louw VJ, Koeffler HP. Cucurbitacin B inhibits growth, arrests the cell cycle, and potentiates antiproliferative efficacy of cisplatin in cutaneous squamous cell carcinoma cell lines. Int J Oncol 2010;37:737–43.
14. Aribi A, Gery S, Lee DH, Thoennissen NH, Thoennissen GB, Alvarez R, et al. The triterpenoid cucurbitacin B augments the antiproliferative activity of chemotherapy in human breast cancer. Int J Cancer 2013;132:2730–7.
15. Zhang M, Sun C, Shan X, Yang X, Li-Ling J, Deng Y. Inhibition of pancreatic cancer cell growth by cucurbitacin B through modulation of signal transducer and activator of transcription 3 signaling. Pancreas 2010;39:923–9.
16. Chan KT, Meng FY, Li Q, Ho CY, Lam TS, To Y, et al. Cucurbitacin B induces apoptosis and S phase cell cycle arrest in BEL-7402 human hepatocellular carcinoma cells and is effective via oral administration. Cancer Lett 2010;294:118–24.
17. Kausar H, Munagala R, Bansal SS, Aqil F, Vadhanam MV, Gupta RC. Cucurbitacin B potently suppresses non-small-cell lung cancer growth: identification of intracellular thiols as critical targets. Cancer Lett 2013;332:35–45.
18. Thoennissen NH, Iwanski GB, Doan NB, Okamoto R, Lin P, Abbassi S, et al. Cucurbitacin B induces apoptosis by inhibition of the JAK/STAT pathway and potentiates antiproliferative effects of gemcitabine on pancreatic cancer cells. Cancer Res 2009;69:5876–84.
19. Zhang Y, Ouyang D, Xu L, Ji Y, Zha Q, Cai J, et al. Cucurbitacin B induces rapid depletion of the G-actin pool through reactive oxygen species-dependent actin aggregation in melanoma cells. Acta Biochim Biophys Sin 2011;43:556–67.
20. Ayyad SE, Abdel-Lateff A, Basaif SA, Shier T. Cucurbitacins-type triterpene with potent activity on mouse embryonic fibroblast from Cucumis prophetarum, cucurbitaceae. Pharmacognosy Res 2011;3:189–93.
21. Meeran SM, Patel SN, Tollefsbol TO. Sulforaphane causes epigenetic repression of hTERT expression in human breast cancer cell lines. PLoS One 2010;5:e11457.

22. Meeran SM, Patel SN, Chan TH, Tollefsbol TO. A novel prodrug of epigallocatechin-3-gallate: differential epigenetic hTERT repression in human breast cancer cells. Cancer Prev Res 2011;4:1243–54.
23. Nikitin AY, Alcaraz A, Anver MR, Bronson RT, Cardiff RD, Dixon D, et al. Classification of proliferative pulmonary lesions of the mouse: recommendations of the mouse models of human cancers consortium. Cancer Res 2004;64:2307–16.
24. Barta P, Van Pelt C, Men T, Dickey BF, Lotan R, Moghaddam SJ. Enhancement of lung tumorigenesis in a Gprc5a Knockout mouse by chronic extrinsic airway inflammation. Mol Cancer 2012;11:4–15.
25. Akhtar S, Meeran SM, Katiyar N, Katiyar SK. Grape seed proanthocyanidins inhibit the growth of human non-small cell lung cancer xenografts by targeting insulin-like growth factor binding protein-3, tumor cell proliferation, and angiogenic factors. Clin Cancer Res 2009;15:821–31.
26. Boisvert FM, Ahmad Y, Gierlin´ski M, Charrière F, Lamont D, Scott M, et al. A Quantitative spatial proteomics analysis of proteome turnover in human cells. Mol Cell Proteomics 2012;11:M111.011429.
27. Reed SI. Ratchets and clocks: the cell cycle, ubiquitylation and protein turnover. Nat Rev Mol Cell Biol 2003;4:855–64.
28. Majid S, Kikuno N, Nelles J, Noonan E, Tanaka Y, Kawamoto K, et al. Genistein induces the p21WAF1/CIP1 and p16INK4a tumor suppressor genes in prostate cancer cells by epigenetic mechanisms involving active chromatin modification. Cancer Res 2008;68:2736–44.
29. Shukla S, Meeran SM. Epigenetic factors in breast cancer progression. In: Ahmad A, editor. Breast cancer metastasis and drug resistance. Springer Publications; New York, 2013. p. 341–65.
30. Li Y, Yuan YY, Meeran SM, Tollefsbol TO. Synergistic epigenetic reactivation of estrogen receptor-alpha (ERalpha) by combined green tea polyphenol and histone deacetylase inhibitor in ERalpha-negative breast cancer cells. Mol Cancer 2010;9:274.
31. Guilleret I, Yan P, Grange F, Braunschweig R, Bosman FT, Benhattar J. Hypermethylation of the human telomerase catalytic subunit (hTERT) gene correlates with telomerase activity. Int J Cancer 2002;101:335–41.
32. Zhu JS, Ouyang DY, Shi ZJ, Xu LH, Zhang YT, He XH. Cucurbitacin B induces cell cycle arrest, apoptosis and autophagy associated with G actin reduction and persistent activation of cofilin in Jurkat cells. Pharmacology 2012;89:348–6.
33. Zhang T, Li Y, Park KA, Byun HS, Won M, Jeon J, et al. Cucurbitacin induces autophagy through mitochondrial ROS production which counteracts to limit caspase-dependent apoptosis. Autophagy 2012;8:559–76.
34. McCool KW, Xu X, Singer DB, Murdoch FE, Fritsch MK. The role of histone acetylation in regulating early gene expression patterns during early embryonic stem cell differentiation. J Biol Chem 2007;282:6696–706.
35. Tang Z, Chen WY, Shimada M, Nguyen UT, Kim J, Sun XJ, et al. SET1 and p300 act synergistically, through coupled histone modifications, in transcriptional activation by p53. Cell 2013;154:297–310.
36. Ducasse M, Brown MA. Epigenetic aberrations and cancer. Mol Cancer 2006;5:60.
37. Kouzarides T. Histone methylation in transcriptional control. Curr Opin Genet Dev 2002;12:198–209.
38. Huang L, Sowa Y, Sakai T, Pardee AB. Activation of the p21WAF1/CIP1 promoter independent of p53 by the histone deacetylase inhibitor suberoylanilide hydroxamic acid (SAHA) through the Sp1 sites. Oncogene 2000;19:5712–9.
39. Xiao H, Hasegawa T, Isobe K. p300 collaborates with Sp1 and Sp3 in p21 (waf1/cip1) promoter activation induced by histone deacetylase inhibitor. J Biol Chem 2000;275:1371–6.
40. Gartel AL, Ye X, Goufman E, Shianov P, Hay N, Najmabadi F, et al. Myc represses the p21(WAF1/CIP1) promoter and interacts with Sp1/Sp3. Proc Natl Acad Sci U S A 2001;98:4510–5.
41. Lin RK, Hsieh YS, Lin P, Hsu HS, Chen CY, Tang YA, et al. The tobacco-specific carcinogen NNK induces DNA methyltransferase 1 accumulation and tumor suppressor gene hypermethylation in mice and lung cancer patients. J Clin Invest 2010;120:521–32.
42. Tang W, Kuruvilla SA, Galitovskiy V, Pan ML, Grando SA, Mukherjee J. Targeting histone deacetylase in lung cancer for early diagnosis: (18)F-FAHA PET/CT imaging of NNK-treated A/J mice model. Am J Nucl Med Mol Imaging 2014;4:324–32.
43. Ecke I, Petry F, Rosenberger A, Tauber S, Mönkemeyer S, Hess I, et al. Antitumor effects of a combined 5-aza-2'deoxycytidine and valproic acid treatment on rhabdomyosarcoma and medulloblastoma in Ptch mutant mice. Cancer Res 2009;69(3):887–95.
44. Tellez CS, Grimes MJ, Picchi MA, Liu Y, March TH, Reed MD, et al. SGI-110 and entinostat therapy reduces lung tumor burden and reprograms the epigenome. Int J Cancer 2014;135:2223–31.
45. Belinsky SA, Swafford DS, Middleton SK, Kennedy CH, Tesfaigzi J. Deletion and differential expression of p16INK4a in mouse lung tumors. Carcinogenesis 1997;18:115–20.